

# Investigations of Non-Physical Characteristic Modes of Material Bodies

SHAODE HUANG<sup>ID</sup>, JIN PAN, AND YUYUE LUO

School of Electronic Science and Engineering, University of Electronic Science and Technology of China, Chengdu 611731, China

Corresponding author: Shaode Huang (shaodehuang@foxmail.com).

**ABSTRACT** Recently, researchers noticed that there are non-physical modes in characteristic modes of material bodies. In this paper, those non-physical modes are investigated. The reason for the non-physical modes is discussed. The influence of integral equations' internal resonance on the non-physical modes are studied. It is concluded that the internal resonance is not responsible for the non-physical modes. Meanwhile, based on the extinction theorem, the dependent relationship between the equivalent surface electric and magnetic currents are proposed, and it is observed that the non-physical modes do not obey the dependent relationship, whereas the physical modes are governed by the dependent relationship. Therefore, it can be concluded that the lack of the dependent relationship causes the non-physical modes. Besides, based on the dependent relationship, a novel post-processing method to remove the non-physical modes is proposed. Numerical results of a dielectric cylinder are presented to validate the discussions and new post-processing method.

**INDEX TERMS** Characteristic modes, non-physical modes, internal resonance, material body, post-processing

## I. INTRODUCTION

The theory of characteristic mode (TCM) is a useful design and analysis tool which determines the electromagnetic properties of a structure only based on its geometry and material properties. The TCM was initially defined by Garbacz [1] and was refined by Harrington and Mautz using the electric field integral equation (EFIE) for perfectly electric conducting (PEC) bodies [2], denoted as EFIE-based CM in this paper. Following the EFIE-based CM, the TCM was extended to material bodies. Harrington *et al.* [3] developed a TCM for material bodies using the volume integral equation (VIE), which is denoted as VIE-based CM in this paper. The VIE-based CM is the first attempt to calculate the characteristic modes (CMs) of material bodies. Although the VIE-based CM provides correct modal solutions for material bodies, it requires an unbearable large number of unknowns when the electric size of material bodies increases. To overcome this problem, Chang and Harrington [4] proposed a TCM for material bodies using the SPMCHWT (symmetric Poggio, Miller, Chang, Harrington, Wu, and Tsai) equation, which will be called as SPMCHWT-based CM in this paper.

However, recently, researchers noticed that the SPMCHWT-based CM could not provide reasonable modal solutions for material bodies. The SPMCHWT-based CM can

also result in many non-physical modes [5]–[12]. Unfortunately, it is still not clear what is responsible for the non-physical modes. Nevertheless, two possible reasons have been proposed [6]–[11]. In [6] Chen and Wang and Chen [7] pointed out that the lack of the dependent relationship between the equivalent surface electric and magnetic currents is the reason behind those non-physical modes in SPMCHWT-based CM. They also proposed two types of formulations—exclusively concerning equivalent surface electric current or magnetic current [6], [7]. However, as [6] and [7] did not give enough convincing proof, their explanation is so far a conjecture. Besides, the formulations proposed in [6] and [7] can still lead to non-physical modes [12]. Therefore, it is necessary to take a new look at the claim of [6] and [7]. Another explanation of the non-physical modes is shown in [8]–[11]. It is pointed out that the SPMCHWT equation suffers from internal resonance problem. The authors deem that the non-physical modes in SPMCHWT-based CM are a direct result of the internal resonance problem. The two types of explanations are quite different, and the origin of the non-physical modes is still ambiguous.

In this paper, the non-physical modes of material bodies are investigated. We calculate the CM based on the APMCHWT

(asymmetric Poggio, Miller, Chang, Harrington, Wu, and Tsai) equation. The CM based on the APMCHWT equation is denoted as APMCHWT-based CM. We should note that the APMCHWT equation is immune from internal resonance [8], [9], [13]. Comparing the results of the SPMCHWT-based CM and the APMCHWT-based CM, we observed that both of the two kinds of CMs suffered from the non-physical modes, which means although the APMCHWT equation is immune from internal resonance, the APMCHWT-based CM still suffers from the non-physical modes. In other words, it can be concluded that the internal resonance is not responsible for the non-physical modes of material bodies. Meanwhile, we propose the dependent relationship between the equivalent surface electric and magnetic currents, as well as a quantifiable indicator to identify whether the equivalent surface electric and magnetic currents obey the dependent relationship. Through plenty of experiments, we can find that the non-physical modes do not obey the dependent relationship, while the physical modes are governed by the dependent relationship. Therefore, we prove that the lack of the dependent relationship causes the non-physical modes of material bodies. Besides, based on the dependent relationship, a novel post-processing method to remove the non-physical modes is proposed in this paper. The proposed theoretical discussions and post-processing method have been validated by numerical results of a dielectric cylinder, which will be presented later.

## II. WHAT CAUSES NON-PHYSICAL MODES?

Chang and Harrington [4] proposed the SPMCHWT-based CM for homogeneous and loss-free material bodies using the following SPMCHWT equation

$$\mathbf{T} \cdot \begin{bmatrix} \vec{J}_s \\ j\vec{M}_s \end{bmatrix} = \begin{bmatrix} \vec{E}_{inc} \\ j\vec{H}_{inc} \end{bmatrix} \quad (1)$$

in which  $\vec{J}_s$  and  $\vec{M}_s$  are the equivalent surface electric and magnetic currents, respectively. The operator  $\mathbf{T}$  are defined as [14]

$$\mathbf{T} = \begin{bmatrix} j\omega\mu\mathbf{L} + j\omega\mu_0\mathbf{L}_0 & -j(\mathbf{K} + \mathbf{K}_0) \\ -j(\mathbf{K} + \mathbf{K}_0) & j\omega\varepsilon\mathbf{L} + j\omega\varepsilon_0\mathbf{L}_0 \end{bmatrix}$$

$$\mathbf{L}_i(\vec{X}) = \left(1 + \frac{1}{k_i^2} \nabla \nabla \cdot\right) \int_{\Omega} G(\vec{r}, \vec{r}', k_i) \vec{X}(\vec{r}') d\Omega'$$

$$\mathbf{K}_i(\vec{X}) = \int_{\Omega} [\nabla G(\vec{r}, \vec{r}', k_i)] \times \vec{X}(\vec{r}') d\Omega' \quad (2)$$

where  $k_i$  is wavenumber, and  $G(\vec{r}, \vec{r}', k_i)$  is the green's function in an unbounded homogeneous medium with the wavenumber  $k_i$ .

Then, Chang and Harrington [4] formulated the SPMCHWT-based CM using the following generalized eigenvalue equation

$$\mathbf{T}_2 \cdot \begin{bmatrix} \vec{J}_n \\ j\vec{M}_n \end{bmatrix} = \lambda_n \mathbf{T}_1 \cdot \begin{bmatrix} \vec{J}_n \\ j\vec{M}_n \end{bmatrix} \quad (3)$$

in which

$$\mathbf{T}_1 = \frac{1}{2} (\mathbf{T} + \mathbf{T}^H)$$

$$\mathbf{T}_2 = \frac{1}{2j} (\mathbf{T} - \mathbf{T}^H) \quad (4)$$

There are some numerical results to validate the SPMCHWT-based CM in [4]. However, [4] displayed only the scattering cross-sections of an infinite circular dielectric cylinder, rather than actual CM eigenvalues, current distributions, and fields. As reported recently, the SPMCHWT-based CM results in non-physical modes [5]–[12]. Unfortunately, the cause of these non-physical modes has not been thoroughly investigated so far. Two types of possible reasons have been proposed recently. In Chen and Wang [6] and Chen [7] pointed out that the lack of the dependent relationship between  $\vec{J}_s$  and  $\vec{M}_s$  causes the non-physical modes in SPMCHWT-based CM. Differently, [8]–[11] claimed that it is the presence of internal resonance of SPMCHWT equation that leads to the non-physical modes.

### A. INTERNAL RESONANCE

In this section, we show that the internal resonance is not responsible for the non-physical modes. Firstly, we consider the APMCHWT-based CM which is based on the following APMCHWT equation

$$\begin{bmatrix} j\omega\mu\mathbf{L} + j\omega\mu_0\mathbf{L}_0 & \mathbf{K} + \mathbf{K}_0 \\ -(\mathbf{K} + \mathbf{K}_0) & j\omega\varepsilon\mathbf{L} + j\omega\varepsilon_0\mathbf{L}_0 \end{bmatrix} \begin{bmatrix} \vec{J}_s \\ \vec{M}_s \end{bmatrix} = \begin{bmatrix} \vec{E}_{inc} \\ \vec{H}_{inc} \end{bmatrix} \quad (5)$$

Except for having different impedance matrices, the approach of formulating the APMCHWT-based CM is very similar to the way to formulate the SPMCHWT-based CM, as shown in (1) - (4). We calculated the numerical results of both the SPMCHWT-based CM and the APMCHWT-based CM of an isolated dielectric cylinder, whose radius is 5.25 mm, height is 4.6 mm, relative permittivity  $\varepsilon_r = 38$ , and relative permeability  $\mu_r = 1$ . The numerical results are calculated using the method of moments. The basis functions and test functions both are RWG (Rao, Wilton, and Glisson) functions [15]. The impedance matrix calculation is based on the method presented in [16]. The accuracy of the impedance matrix calculation depends on the singularity treatment in the calculation of diagonal and near-diagonal elements. In this paper, the singularity treatment is based on the method described in [17], which is proved to be very effective.

Before comparing the results of the two types of CMs, we briefly review the definition of an important parameter, the modal significance (MS). The MS is defined as

$$MS = \left| \frac{1}{1 + j\lambda} \right| \quad (6)$$

in which  $\lambda$  is characteristic value. Both of the MS and characteristic value are the intrinsic properties of CMs and are independent of any specific external source. However, in general, the MS is more convenient than  $\lambda$  to investigate the

resonant behavior over a wide frequency band, because the MS transforms the  $[-\infty, +\infty]$  range of  $\lambda$  into a smaller range of  $[0, 1]$ . Therefore, rather than characteristic value, we will show the results of MS for its simplicity.

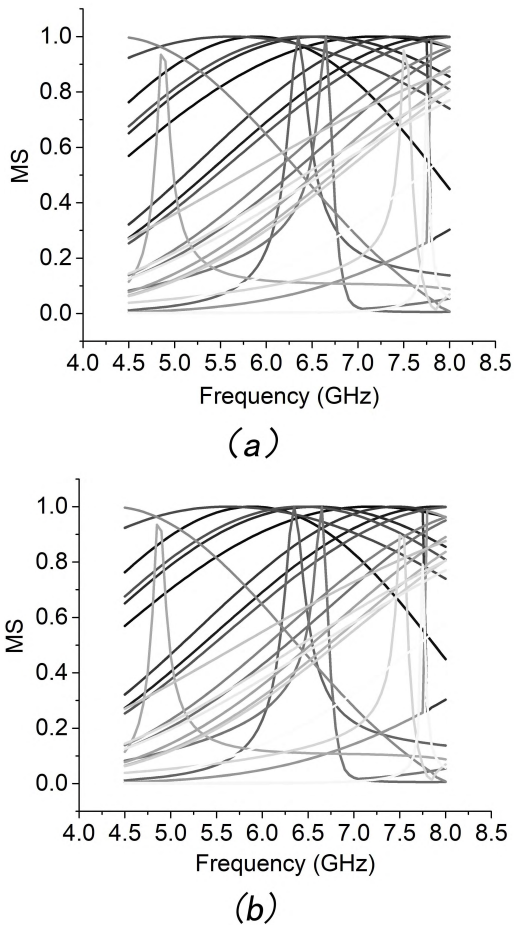


FIGURE 1. MS of the first 30 modes. (a) SPMCHWT-based CM. (b) APMCHWT-based CM.

Firstly, Fig. 1 plots the MS of the first 30 modes solved from the SPMCHWT-based CM and the APMCHWT-based CM. Note that the lines are differentiated by colors than labels, as a compromise to display the 30 lines more clearly. The grayscale value of each line is increasing according to the increment of the modes order: Lines with dark color represent the lower order modes, and lines with light color represent the higher order modes. Fig. 1 illustrate that the MS of the two kinds of CMs are identical. As the non-physical modes in SPMCHWT-based CM have been verified in [5]–[12], we can infer that the APMCHWT-based CM suffers from the non-physical modes even though the APMCHWT equation is immune from internal resonance.

Secondly, Sarkar *et al.* [18] pointed out that the EFIE-based CM of PEC bodies only breaks down at internal resonant frequencies. The SPMCHWT equation suffers from internal resonance only at some discrete frequencies [19]. Therefore, the non-physical modes should only appear at some discrete

frequencies if we assume that internal resonance is responsible for the non-physical modes of material bodies. However, as shown in Fig. 1, the SPMCHWT-based CM of material bodies breaks down at all frequencies, *i.e.*, the non-physical modes appear at all frequencies.

Thirdly, it has been verified that the EFIE for closed PEC bodies suffers from internal resonance [19]. However, the EFIE-based CM provides correct modal solutions even for closed PEC bodies such as sphere [6]. Therefore, it can be inferred that there is no specific relationship between internal resonance and non-physical modes.

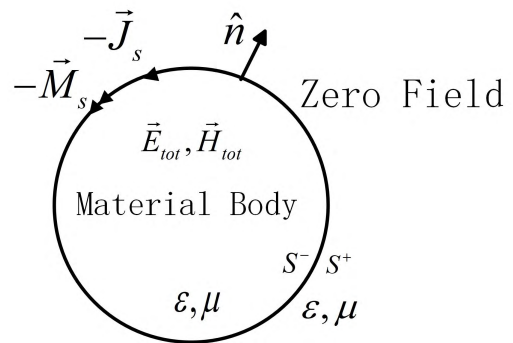


FIGURE 2. Extinction theorem.

In summary, the internal resonance is not responsible for the non-physical modes.

### B. DEPENDENT RELATIONSHIP BETWEEN EQUIVALENT SURFACE ELECTRIC AND MAGNETIC CURRENTS

According to the extinction theorem [19],  $\vec{J}_s$  and  $\vec{M}_s$  are dependent, which means when  $\vec{J}_s$  is solved,  $\vec{M}_s$  can be obtained using  $\vec{J}_s$ , and vice versa. The specific dependent relationship between  $\vec{J}_s$  and  $\vec{M}_s$  can be derived through the extinction theorem as Fig. 2 and (7) show

$$\begin{aligned} -j\omega\mu\mathbf{L}(-\vec{J}_s) - \mathbf{K}(-\vec{M}_s) &= 0, \quad r \in S^+ \\ -j\omega\epsilon\mathbf{L}(-\vec{M}_s) + \mathbf{K}(-\vec{J}_s) &= 0, \quad r \in S^+ \end{aligned} \quad (7)$$

where  $S^+$  denotes the external surface of material body. As can be observed from (7), the dependent relationship only depends on the shape and constitutive parameters of material bodies, and it is unrelated to the excitation sources and background media.

When calculating the SPMCHWT-based CM,  $\vec{J}_s$  and  $\vec{M}_s$  are obtained simultaneously. It is questionable whether  $\vec{J}_s$  and  $\vec{M}_s$  obey the dependent relationship which were described in (7). How to identify whether  $\vec{J}_s$  and  $\vec{M}_s$  obey the dependent relationship is a challenging problem, especially when there are a large number of CMs. It is necessary to propose a quantifiable indicator to simplify the recognition procedure.

We denote the  $\vec{M}_s$  obtained using the dependent relationship as  $\vec{M}_s'(\vec{J}_s)$ , and the  $\vec{J}_s$  obtained using the dependent relationship as  $\vec{J}_s'(\vec{M}_s)$ . For convenience, we define the

symmetric product of two vector functions  $\vec{A}$  and  $\vec{B}$  in  $\Omega$  as

$$\langle \vec{A}, \vec{B} \rangle_{\Omega} = \int_{\Omega} \vec{A} \cdot \vec{B} d\Omega \quad (8)$$

Then the correlation coefficient between  $\vec{J}_s$  and  $\vec{J}'_s (\vec{M}_s)$  is given by following equations

$$\rho_J = \rho_{JA} \cdot \rho_{JD} \quad (9)$$

$$\rho_{JA} = \min \left\{ \frac{\langle \vec{J}_s, \vec{J}_s \rangle_S}{\langle \vec{J}'_s (\vec{M}_s), \vec{J}'_s (\vec{M}_s) \rangle_S}, \frac{\langle \vec{J}'_s (\vec{M}_s), \vec{J}'_s (\vec{M}_s) \rangle_S}{\langle \vec{J}_s, \vec{J}_s \rangle_S} \right\} \quad (10)$$

$$\rho_{JD} = \frac{|\langle \vec{J}_s, \vec{J}'_s (\vec{M}_s) \rangle_S|}{\sqrt{\langle \vec{J}_s, \vec{J}_s \rangle_S} \cdot \sqrt{\langle \vec{J}'_s (\vec{M}_s), \vec{J}'_s (\vec{M}_s) \rangle_S}} \quad (11)$$

where  $\rho_{JA}$  indicates the correlation of amplitude,  $\rho_{JD}$  indicates the correlation of distribution, and  $\min$  means to select the smaller value. Similarly, the correlation coefficient between  $\vec{M}_s$  and  $\vec{M}'_s (\vec{J}_s)$  is given by following equations

$$\rho_M = \rho_{MA} \cdot \rho_{MD} \quad (12)$$

$$\rho_{MA} = \min \left\{ \frac{\langle \vec{M}_s, \vec{M}_s \rangle_S}{\langle \vec{M}'_s (\vec{J}_s), \vec{M}'_s (\vec{J}_s) \rangle_S}, \frac{\langle \vec{M}'_s (\vec{J}_s), \vec{M}'_s (\vec{J}_s) \rangle_S}{\langle \vec{M}_s, \vec{M}_s \rangle_S} \right\} \quad (13)$$

$$\rho_{MD} = \frac{|\langle \vec{M}_s, \vec{M}'_s (\vec{J}_s) \rangle_S|}{\sqrt{\langle \vec{M}_s, \vec{M}_s \rangle_S} \cdot \sqrt{\langle \vec{M}'_s (\vec{J}_s), \vec{M}'_s (\vec{J}_s) \rangle_S}} \quad (14)$$

It is obvious that  $\rho_J$  and  $\rho_M$  have a range of [0, 1]. When  $\rho_J$  or  $\rho_M$  approaches to unit,  $\vec{J}_s$  and  $\vec{M}_s$  obey the dependent relationship. The extent of approximation can be quantifiable via a given threshold value. In other words, when  $\rho_J$  or  $\rho_M$  is above the given threshold value,  $\vec{J}_s$  and  $\vec{M}_s$  obey the dependent relationship. According to mass computation results, setting the threshold value as 0.9 is acceptable.

Considering the same dielectric cylinder mentioned above, we compute  $\rho_J$  and  $\rho_M$  of the first 30 modes of the SPMCHWT-based CM at 4.5 GHz and 5.0 GHz, as displayed in Fig. 3. In Fig. 3, we can observe that there are only five modes which are governed by the dependent relationship. The indexes of the five modes are 15, 16, 17, 19, and 27.

Fig. 4 demonstrates the radiated powers of the first 30 modes of SPMCHWT-based CM at 4.5 GHz and 5.0 GHz. Note that all CMs have been normalized using (27) in [4]. According to the observations in [5], the modes whose radiation power does not equal to 1W are the non-physical modes. Comparing Fig. 3 with Fig. 4, it can be concluded that

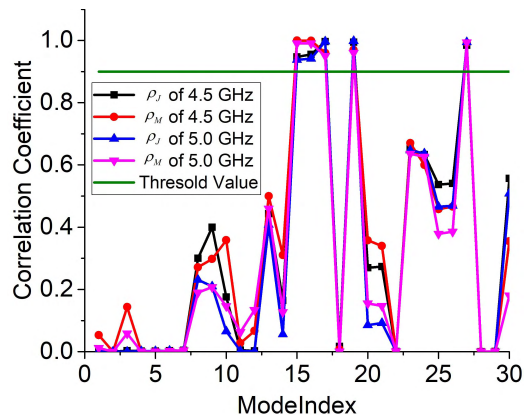


FIGURE 3.  $\rho_J$  and  $\rho_M$  of first 30 SPMCHWT-based CMs.

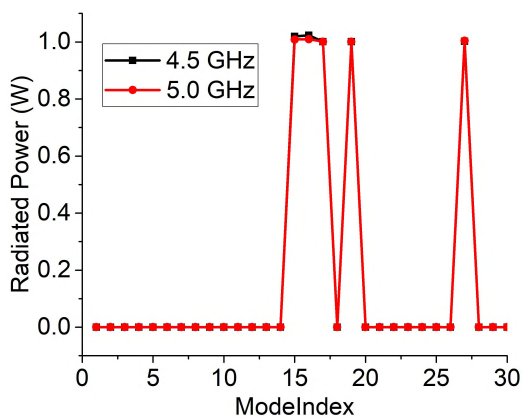


FIGURE 4. Radiated Power of first 30 SPMCHWT-based CMs.

the modes governed by the dependent relationship are the physical modes, whereas those do not obey the dependent relationship are the non-physical modes.

To vividly display the difference between the non-physical modes and the physical modes, we plot  $\vec{J}_s$ ,  $\vec{M}_s$ ,  $\vec{J}'_s (\vec{M}_s)$ , and  $\vec{M}'_s (\vec{J}_s)$  of two non-physical modes and two physical modes at 4.5 GHz. The current distributions are shown in Fig. 5 to 8. All currents have been normalized to its maximum value to facilitate comparison. Taking mode 1 as an example, we can see its actual electric current distribution in Fig. 5(a). As a comparison, Fig. 5(c) displays mode 1's electric current distribution calculated by the magnetic current and dependent relationship. Similarly, Fig. 5(b) illustrates the actual magnetic current distribution of mode 1, whereas mode 1's magnetic current distribution calculated by the electric current and dependent relationship are shown in Fig. 5(d). If the electric and magnetic currents of mode 1 obey the dependent relationship, Fig. 5(a) and Fig. 5(b) should be identical to Fig. 5(c) and Fig. 5(d), respectively. We can apply the similar analysis to Fig. 6 to 8. It can be clearly observed from Fig. 5 to 8 that  $\vec{J}_s$  and  $\vec{M}_s$  of the non-physical modes do not obey the dependent relationship, while  $\vec{J}_s$  and  $\vec{M}_s$  of the physical modes obey the dependent relationship.

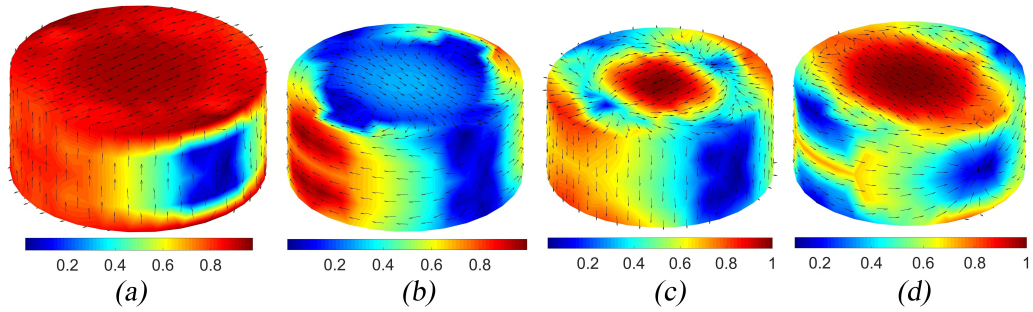


FIGURE 5. Current distributions of mode 1 (non-physical). (a)  $\vec{J}_s$ . (b)  $\vec{M}_s$ . (c)  $\vec{J}'_s(\vec{M}_s)$ . (d)  $\vec{M}'_s(\vec{J}_s)$ .

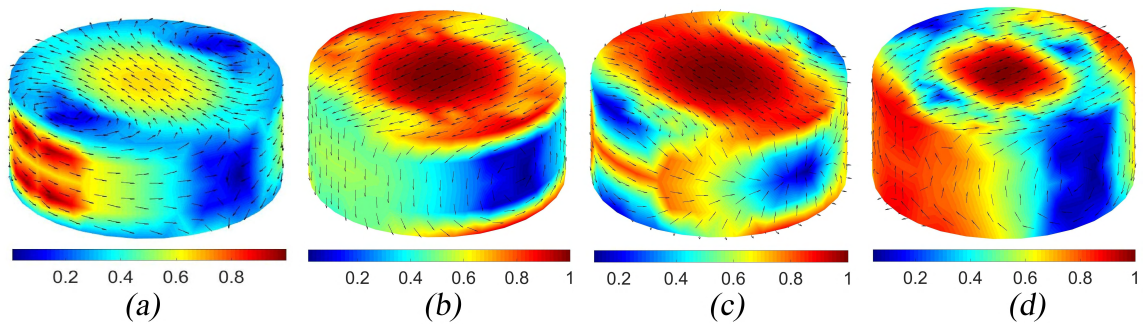


FIGURE 6. Current distributions of mode 2 (non-physical). (a)  $\vec{J}_s$ . (b)  $\vec{M}_s$ . (c)  $\vec{J}'_s(\vec{M}_s)$ . (d)  $\vec{M}'_s(\vec{J}_s)$ .

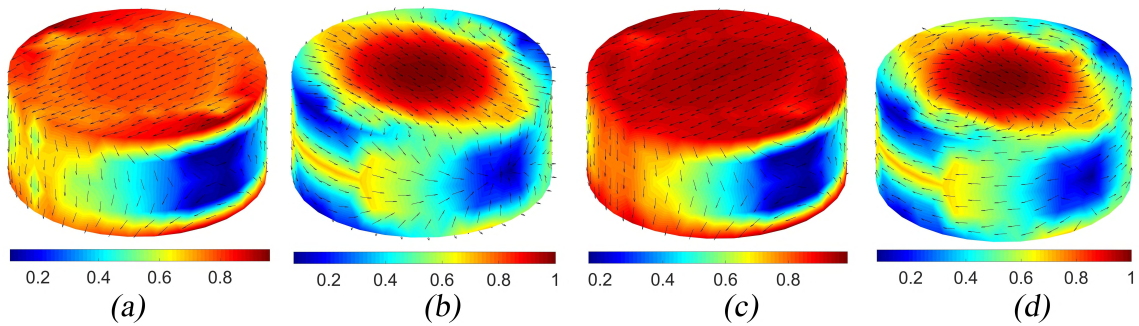


FIGURE 7. Current distributions of mode 15 (physical). (a)  $\vec{J}_s$ . (b)  $\vec{M}_s$ . (c)  $\vec{J}'_s(\vec{M}_s)$ . (d)  $\vec{M}'_s(\vec{J}_s)$ .

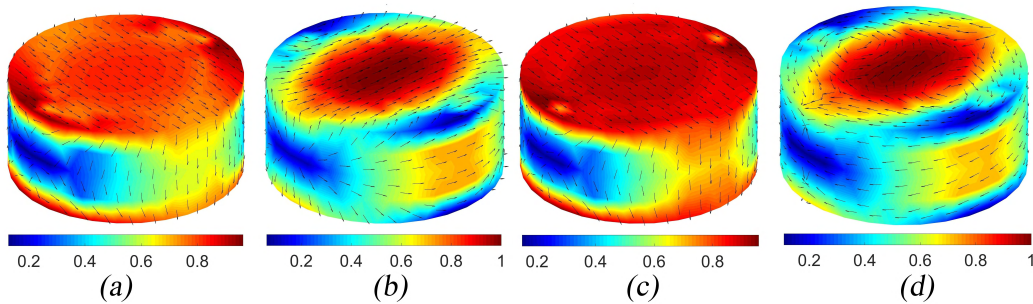


FIGURE 8. Current distributions of mode 16 (physical). (a)  $\vec{J}_s$ . (b)  $\vec{M}_s$ . (c)  $\vec{J}'_s(\vec{M}_s)$ . (d)  $\vec{M}'_s(\vec{J}_s)$ .

In summary, the lack of the dependent relationship between  $\vec{J}_s$  and  $\vec{M}_s$  causes non-physical modes of material bodies, and the internal resonance is not responsible for the non-physical modes.

### III. REMOVE NON-PHYSICAL MODES

In this section, based on the dependent relationship, we propose a novel post-processing method to remove the non-physical modes.

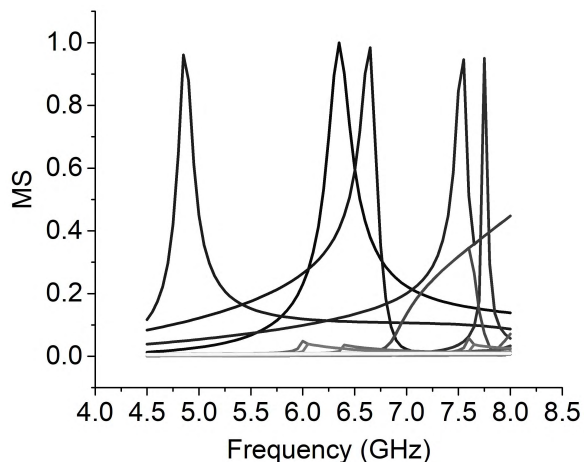


FIGURE 9. MS of the first 30 CMs after post-processing.

As mentioned above, when  $\rho_J$  or  $\rho_M$  is above the given threshold value, the corresponding mode is a physical mode. Therefore, after calculating and tracking CMs at sampling frequencies, we should check  $\rho_J$  or  $\rho_M$  of all CMs at one frequency. As long as all CMs are tracked correctly, if a mode is identified as non-physical at one frequency, then the mode is non-physical over the whole frequency band. That is to say, the checking procedure is only carried out at one frequency, rather than all sampling frequencies. After comparing  $\rho_J$  or  $\rho_M$  with the threshold value, the physical modes at one frequency can be recognized. As the correct tracking procedure has been done before the checking procedure, the physical modes at all sampling frequencies can be identified. Compared with previous post-processing method [10], the new method does not need to recalculate CMs at all sampling frequencies. Therefore, the new method can save the post-processing time.

To validate the new post-processing method, we consider the SPMCHWT-based CM of the same dielectric cylinder mentioned above. Before the post-processing, the MS of the first 30 CMs is illustrated in Fig. 1. After implementing the proposed post-processing method, the MS of the first 30 CMs is shown in Fig. 9. It can be observed that there are only five resonant frequencies (the resonant frequencies can be obtained through locating the peak of MS), 4.87 GHz, 6.35 GHz, 6.65 GHz, 7.55 GHz, and 7.77 GHz. The resonant frequencies agree well with those obtained from the determinant root seeking method in [20]. Therefore, the results validate the proposed post-processing method.

#### IV. CONCLUSION

In this paper, we have studied the reason for the non-physical modes in SPMCHWT-based CM of material bodies. We find that the internal resonance is not responsible for the non-physical modes, and the lack of the dependent relationship between the equivalent surface electric and magnetic currents causes the non-physical modes. Besides, based on the dependent relationship, we propose a novel post-processing method, which has been proved to be very effective to remove the non-physical modes.

#### LIST OF ACRONYMS

CM	characteristic mode
TCM	theory of characteristic mode
EFIE	electric field integral equation
PEC	perfectly electric conducting
VIE	volume integral equation
PMCHWT	Poggio, Miller, Chang, Harrington, Wu, Tsai
SPMCHWT	symmetric PMCHWT
APMCHWT	asymmetric PMCHWT
RWG	Rao, Wilton, and Glisson
MS	modal significance

#### REFERENCES

- [1] R. J. Garbacz, "Modal expansions for resonance scattering phenomena," *Proc. IEEE*, vol. 53, no. 8, pp. 856–864, Aug. 1965.
- [2] R. F. Harrington and J. R. Mautz, "Theory of characteristic modes for conducting bodies," *IEEE Trans. Antennas Propag.*, vol. 19, no. 5, pp. 622–628, Sep. 1971.
- [3] R. F. Harrington, J. R. Mautz, and Y. Chang, "Characteristic modes for dielectric and magnetic bodies," *IEEE Trans. Antennas Propag.*, vol. 20, no. 2, pp. 194–198, Mar. 1972.
- [4] Y. Chang and R. F. Harrington, "A surface formulation for characteristic modes of material bodies," *IEEE Trans. Antennas Propag.*, vol. 25, no. 6, pp. 789–795, Nov. 1977.
- [5] H. Alroughani, J. L. T. Ethier, and D. A. McNamara, "Observations on computational outcomes for the characteristic modes of dielectric objects," in *Proc. IEEE Antennas Propag. Soc. Int. Symp. (APSURSI)*, Jul. 2014, pp. 844–845.
- [6] Y. Chen and C.-F. Wang, *Characteristic Modes: Theory and Applications in Antenna Engineering*. New York, NY, USA: Wiley, 2015.
- [7] Y. Chen, "Alternative surface integral equation-based characteristic mode analysis of dielectric resonator antennas," *IET Microw., Antennas Propag.*, vol. 10, no. 2, pp. 193–201, 2016.
- [8] Z. T. Miers and B. K. Lau, "Computational analysis and verifications of characteristic modes in real materials," *IEEE Trans. Antennas Propag.*, vol. 64, no. 7, pp. 2595–2607, Jul. 2016.
- [9] Z. T. Miers and B. K. Lau, "Effects of dielectrics and internal resonances on modal analysis of terminal chassis," in *Proc. 10th Eur. Conf. Antennas Propag. (EuCAP)*, Apr. 2016, pp. 1–5.
- [10] Z. Miers and B. K. Lau, "Post-processing removal of non-real characteristic modes via basis function perturbation," in *Proc. IEEE Int. Symp. Antennas Propag. (APSURSI)*, Jul. 2016, pp. 419–420.
- [11] Z. Miers and B. K. Lau, "On characteristic eigenvalues of complex media in surface integral formulations," *IEEE Antennas Wireless Propag. Lett.*, vol. 16, pp. 1820–1823, Mar. 2017.
- [12] R. Lian, J. Pan, and S. Huang, "Alternative surface integral equation formulations for characteristic modes of dielectric and magnetic bodies," *IEEE Trans. Antennas Propag.*, vol. 65, no. 9, pp. 4706–4716, Sep. 2017.
- [13] J. R. Mautz and R. F. Harrington, "Electromagnetic scattering from a homogeneous body of revolution," Dept. Elect. Comput. Eng., Syracuse Univ., New York, NY, USA, 1977.
- [14] W. C. Gibson, *The Method of Moments in Electromagnetics*. Boca Raton, FL, USA: CRC press, 2014.
- [15] S. M. Rao, D. R. Wilton, and A. W. Glisson, "Electromagnetic scattering by surfaces of arbitrary shape," *IEEE Trans. Antennas Propag.*, vol. 30, no. 3, pp. 409–418, May 1982.
- [16] R. F. Harrington and J. R. Mautz, "Computation of characteristic modes for conducting bodies," *IEEE Trans. Antennas Propag.*, vol. 19, no. 5, pp. 629–639, Sep. 1971.
- [17] P. Yla-Oijala and M. Taskinen, "Calculation of cfie impedance matrix elements with rwg and  $n \times rwg$  functions," *IEEE Trans. Antennas Propag.*, vol. 51, no. 8, pp. 1837–1846, Aug. 2003.
- [18] T. K. Sarkar, E. L. Mokole, and M. Salazar-Palma, "An expose on internal resonance, external resonance, and characteristic modes," *IEEE Trans. Antennas Propag.*, vol. 64, no. 11, pp. 4695–4702, Nov. 2016.

- [19] W. C. Chew, M. S. Tong, and B. Hu, "Integral equation methods for electromagnetic and elastic waves," *Synth. Lect. Comput. Electromagn.*, vol. 3, no. 1, pp. 1–241, 2008.
- [20] D. Kajfez, A. W. Glisson, and J. James, "Computed modal field distributions for isolated dielectric resonators," *IEEE Trans. Microw. Theory Techn.*, vol. 32, no. 12, pp. 1609–1616, Dec. 1984.



**SHAODE HUANG** was born in Sichuan, China, in 1992. He received the B.S. degree in electromagnetic field and microwave technique from the University of Electronic Science and Technology of China, Chengdu, China, in 2014, where he is currently pursuing the Ph.D. degree. His current research interests include the theory of characteristic mode, computational electromagnetics, and antenna theory.



**JIN PAN** received the B.S. degree in electronics and communication engineering from the Radio Engineering Department, Sichuan University, Chengdu, China, in 1983, and the M.S. and Ph.D. degrees in electromagnetic field and microwave technique from the University of Electronic Science and Technology of China (UESTC), in 1983 and 1986, respectively. From 2000 to 2001, he was a Visiting Scholar in electronics and communication engineering with the Radio Engineering Department, City University of Hong Kong. He is currently a Full Professor with the School of Electronic Engineering, UESTC. His current research interests include electromagnetic theory and computation, antenna theory and technique, field and wave in inhomogeneous media, and microwave remote sensing theory and its applications.



**YUYUE LUO** was born in Sichuan, China, in 1991. She received the B.S. degree in electromagnetic field and microwave technique from the University of Electronic Science and Technology of China, Chengdu, China, in 2013, where she is currently pursuing the Ph.D. degree. Her current research interests include antenna theory and array signal processing.

...